

**Prediction of Time-Dependent CYP3A4 Drug-Drug Interactions – Impact of Enzyme  
Degradation, Parallel Elimination Pathways and Intestinal Inhibition**

Aleksandra Galetin, Howard Burt, Laura Gibbons and J. Brian Houston

School of Pharmacy and Pharmaceutical Sciences, University of Manchester, Oxford  
Road, Manchester, M13 9PL, United Kingdom

Running title: Prediction of time-dependent CYP3A4 drug-drug interactions

**Corresponding author:** Dr A. Galetin  
School of Pharmacy and Pharmaceutical Sciences,  
University of Manchester,  
Oxford Road,  
Manchester, M13 9PL, UK  
Tel: (+) 44 161 275 6886  
Fax: (+) 44 161 275 8349  
Email: [Aleksandra.Galetin@manchester.ac.uk](mailto:Aleksandra.Galetin@manchester.ac.uk)

Text: 28  
Tables: 5  
Figures: 6  
References: 40  
Abstract: 243  
Introduction: 708  
Discussion: 1461

**Abbreviations used are:** TDI, time-dependent drug-drug interaction(s); AUC, area under the plasma concentration-time curve; AUC<sub>i</sub>, area under the curve in the presence of the inhibitor; F<sub>G</sub>, intestinal wall availability; F<sub>G</sub><sup>'</sup>, intestinal wall availability in the presence of an inhibitor; k<sub>inact</sub>, maximal inactivation rate constant; K<sub>I</sub>, inhibitor concentration at 50% of k<sub>inact</sub>; f<sub>mCYP3A4</sub>, fraction of victim drug metabolized by CYP3A4; k<sub>deg</sub>, enzyme degradation rate constant; t<sub>1/2deg</sub>, degradation half-life.

## ABSTRACT

Time-dependent inhibition of CYP3A4 often results in clinically significant drug-drug interactions. In the current study, 37 *in vivo* cases of irreversible inhibition were collated, focusing on macrolides (erythromycin, clarithromycin and azithromycin) and diltiazem as inhibitors. The interactions included 17 different CYP3A substrates showing up to 7-fold increase in AUC (13.5 % of studies were in the range of potent inhibition). A systematic analysis of the impact of CYP3A4 degradation half-life (mean  $t_{1/2\text{deg}}=3$  days, ranging from 1-6 days) on the prediction of the extent of interaction for compounds with a differential contribution from CYP3A4 to the overall elimination (defined by  $f_{\text{mCYP3A4}}$ ) was performed. Although the prediction accuracy was very sensitive to CYP3A4 degradation rate for substrates mainly eliminated by this enzyme ( $f_{\text{mCYP3A4}} \geq 0.9$ ), minimal effects are observed when CYP3A4 contributes less than 50% to the overall elimination in cases when the parallel elimination pathway is not subject to inhibition. Use of the mean CYP3A4  $t_{1/2\text{deg}}$  (3 days), average unbound systemic plasma concentration of the inhibitor and the corresponding  $f_{\text{mCYP3A4}}$  resulted in 89% studies predicted within 2-fold of the *in vivo* value. The impact of the interaction in the gut wall was assessed by assuming maximal intestinal inhibition of CYP3A4. Although a reduced number of false negative predictions was observed there was an increased number of over-predictions, and generally a loss of prediction accuracy was observed. The impact of the possible interplay between CYP3A4 and efflux transporters on the intestinal interaction requires further evaluation.

As the most abundant human P450 enzyme in both liver and intestine, CYP3A4 is susceptible to a number of reversible and irreversible metabolic drug-drug interactions. Irreversible, often referred to as mechanism-based, inhibition interactions involve the metabolism of an inhibitor by CYP3A4 to a reactive metabolite which inactivates the catalysing enzyme in a concentration- and time-dependent manner (Silverman, 1995). A key characteristic of this type of inhibition is that inactivation occurs without the release of the reaction product from the catalytic site (Kent et al., 2001). The interaction between the inactivating species and enzyme can either be covalent or non-covalent, involving binding to protein or haeme moiety, respectively (Zhou et al., 2005).

The two major kinetic parameters that characterize time-dependent inhibition interactions (TDI) are  $k_{\text{inact}}$  and  $K_i$ , the maximal inactivation rate constant and the inhibitor concentration leading to 50% of  $k_{\text{inact}}$ , respectively (Silverman, 1995). The  $k_{\text{inact}}/K_i$  ratio is commonly taken as an indicator of the in vitro potency of a mechanism-based inhibitor. The methods used to obtain  $k_{\text{inact}}$  and  $K_i$  estimates generally vary across studies; the CYP3A4 probes used (midazolam, testosterone or triazolam), their concentration (from below the  $K_m$  to the concentrations equivalent to  $V_{\text{max}}$ ), pre-incubation to incubation time ratio and data analysis method employed, all of which may affect the estimates of inhibitor potency.

Quantitative in vitro-in vivo drug interaction prediction work has focused mainly on reversible interactions, whereas TDI were assessed on an individual case-to-case basis (Ito et al., 2003, Wang et al., 2004). In contrast to reversible inhibition, CYP3A4 activity can only be restored by synthesis of new enzyme, often resulting in significant clinical interactions. General under-prediction of an observed TDI using the simple  $[I]/K_i$  approach (Ito et al., 2004, Rostami and Tucker, 2004) indicated a need for a more systematic analysis of this type of inhibition interaction.

The theoretical background for the quantitative prediction of TDI, incorporating the contribution of both hepatic and intestinal interaction, has been described previously (Wang et al., 2004) and was applied here (see Methods). The aim of the current study was to investigate systematically the significance of a number of parameters on the prediction of TDI, namely

enzyme degradation rate, the differential contribution of CYP3A4 to the victim drug elimination and the effect of intestinal inhibition. Assessment was performed on 37 selected in vivo studies with macrolides (azithromycin, clarithromycin and erythromycin) and diltiazem; the metric used was the  $AUC_i/AUC$  ratio for the plasma concentration-time profiles in the presence and absence of the inhibitor, respectively, in agreement with previous analyses (Tucker et al., 2001, Galetin et al., 2005). The rationale for selection of these 4 inhibitors was the availability of both in vitro data and a wide range of in vivo interactions (including 17 different substrates with a differential contribution of CYP3A4 and renal excretion to their elimination). In addition, the prediction accuracy of this mechanistic approach was compared to the predictions based solely on reversible inhibition.

The rate of change of active enzyme concentration is determined by the equilibrium between the rates of de novo synthesis and degradation of the enzyme. Previous predictions of TDI (Ito et al., 2003, Wang et al., 2004) used CYP3A4 degradation half-life estimates ( $t_{1/2deg}$ ) obtained in either rat or Caco-2 cells (Correia, 1991, Malhotra et al., 2001), resulting in  $t_{1/2deg}$  of 14-35 hrs. In the current study we have used estimates of human CYP3A4  $k_{deg}$  from both induction studies or from in vitro investigations in liver slices. The impact of inter-individual variability (estimated CYP3A4  $t_{1/2deg}$  varied from 1-6 days) on the prediction of TDI was assessed in addition to the fraction of the victim drug metabolised by CYP3A4 (defined by  $f_{m_{CYP3A4}}$ ) as this parameter has been shown to have a significant impact on the drug-drug interaction prediction accuracy (Brown et al., 2005, Galetin et al., 2005, Ito et al., 2005.).

Significant intestinal first-pass metabolism may contribute to the inter-individual variability observed in bioavailability and extent of drug-drug interactions for some CYP3A4 substrates. Therefore, the effect of assuming maximal intestinal inhibition on the precision and accuracy of the TDI predictions was investigated in conjunction with the detailed inhibitor- and substrate-related information (e.g., different inhibitor concentrations and parallel elimination pathways, respectively). The implications of maximal intestinal inhibition for drug elimination involving both metabolism and transporters are discussed.

## Materials and Methods

**In vivo studies.** In the current analysis, 37 clinical studies of irreversible inhibition have been collated focusing on macrolides (erythromycin, clarithromycin and azithromycin) and diltiazem as time-dependent inhibitors of CYP3A4. The increase in the area under plasma concentration-time profile in the presence of the inhibitor relative to control ( $AUC_i/AUC$ ) has been used as the metric to assess the degree of interaction. In the case of replicate studies (same dose of the inhibitor) the weighted mean of the AUC ratios was obtained for further analysis, as described previously (Galetin et al., 2005). Drug-drug interaction data resulting after the multiple dosing of an inhibitor and simultaneous oral administration of both drugs were used; studies selected involved 17 different CYP3A4 substrates (Table 1). In addition, clinical data on verapamil, mibefradil, saquinavir and ritonavir interactions ( $n=15$ ) were collated for comparative reasons; no predictions were performed for these inhibitors.

**In vitro data.** Critical assessment of the available in vitro data was performed and the estimates obtained in studies with the most appropriate experimental design (Ghanbari et al., submitted for publication) were used for prediction. The main focus was on the pre-incubation to incubation time ratio ( $>1$ ), use of dilution factor from the pre-incubation to the incubation stage (ideally 1:10 to reduce the occurrence of competitive inhibition between the inhibitor and marker substrate in the second incubation), use of high substrate concentrations (equivalent to  $V_{max}$ ) and non-linear regression analysis for obtaining the  $k_{inact}$  and  $K_I$  parameters. The  $k_{inact}$  and  $K_I$  estimates selected (Table 2) were obtained in the pooled human liver microsomes using either midazolam (macrolides, Ito et al., 2003) or testosterone (diltiazem, Rowland Yeo and Yeo, 2001) as the in vitro probe, whereas the estimates for N-desmethyldiltiazem were obtained by spectroscopic measurements of the metabolite intermediate complex formation (Mayhew et al., 2000). No correction for microsomal binding was employed for macrolides and N-desmethyldiltiazem, whereas microsomal fraction unbound of 0.61 was used for diltiazem (calculated using equation defined by Austin et al., 2002 and logP value of 2.7 obtained by Wang et al., 1997).

**Prediction of time-dependent drug interactions.** The extent of time-dependent inhibition interaction incorporating the contribution of parallel elimination pathways (other P450 enzymes or renal clearance, defined by  $1-f_{mCYP3A4}$ ) was predicted using the following equation (Wang et al., 2004):

$$\frac{AUC'_{po}}{AUC_{po}} = \frac{F_G'}{F_G} \times \frac{1}{\frac{f_{mCYP3A4}}{1 + \sum_{i=1}^n \frac{k_{inact,i} \times I_{u,i}}{K_{L,u} + I_{u,i}}} + (1 - f_{mCYP3A4})} \quad (1)$$

where  $k_{inact}$  represents the maximal inactivation rate constant,  $K_i$  is the inhibitor concentration at 50% of  $k_{inact}$ ,  $I_u$  is the unbound inhibitor concentration (either the average systemic plasma concentration after repeated oral administration ( $[I]_{av}$ ), or the maximum hepatic input concentration ( $[I]_{in}$ ), (taken from Ito et al., 2004, range shown in Table 2),  $f_{mCYP3A4}$  is the fraction of victim drug metabolized by CYP3A4,  $k_{deg}$  is the endogenous degradation rate constant of the enzyme,  $F_G'$  and  $F_G$  are the intestinal wall availability in the presence and absence of inhibitor, respectively. Absorption rate constants used to obtain the  $[I]_{in}$  values for erythromycin, clarithromycin, azithromycin and diltiazem were 0.011, 0.018, 0.00175 and 0.039  $\text{min}^{-1}$ , whereas the unbound fractions to the plasma protein were 0.16, 0.7, 0.28 and 0.175, respectively (Echizen and Eichelbaum, 1986, Ito et al., 2003). The impact of N-desmethyldiltiazem, an active metabolite of diltiazem, on the predicted degree of interaction was investigated assuming the same plasma protein binding as for diltiazem and the relative plasma concentration is 38% of the parent (Echizen and Eichelbaum, 1986).

Values for  $f_{mCYP3A4}$  were taken from Brown et al. (2005), Galetin et al. (2005) and Egnell et al. (2003) (carbamazepine); cyclosporine values were generated by regression analysis using eq. 1, as described previously (Ito et al., 2005). For loratadine, terfenadine and nitrazepam the number of studies was limited and the  $f_{mCYP3A4}$  was obtained by the rank order approach using studies with midazolam and the same dose of erythromycin as applied previously (Brown et al., 2005).

Human CYP3A degradation constants were collated from induction studies with carbamazepine, ritonavir, rifampin and in vitro studies, as shown in Table 3. The impact of

the different  $k_{deg}$  values (0.0005-0.00008  $\text{min}^{-1}$ , corresponding to CYP3A4  $t_{1/2deg} = 1-6$  days) on the predicted AUC ratio was assessed for cases with an increasing contribution of CYP3A4 to the overall elimination ( $fm_{CYP3A4} = 0.4-1$ ). This was carried out both by simulation at a constant or a range of inhibitor concentrations and by assessing the precision and accuracy of the predicted  $AUC_i/AUC$  (see below). In addition, simulations of the effects of the multiple time-dependent inhibitors were performed assuming that the inhibitors inhibit the same enzyme, i.e., act via the same mechanism. The simulations investigated the scenarios where the second inhibitor is either equipotent or 5, 10 and 50-fold more potent (greater  $k_{inact}/K_I$  ratio) than the first inhibitor, for different  $fm_{CYP3A4}$  values.

The contribution of the enzyme interaction in the intestinal wall was evaluated by incorporating the ratio of intestinal wall availability in the presence and absence of inhibitor,  $F_G'$  and  $F_G$ , respectively into the hepatic prediction (Wang et al., 2004), as shown in eq. 1. The impact of the maximal inhibition of intestinal metabolism in the presence of the inhibitor ( $F_G' = 1$ ) on the prediction of TDI was assessed. The  $F_G$  control values for the corresponding substrates were obtained indirectly from oral and iv administration data assuming complete absorption, negligible intestinal metabolism after iv administration and that the systemic clearance of a drug after iv dose reflects only hepatic elimination (eqs. 2-3) (Hall et al., 1999)

$$F = F_{abs} (1 - E_G) (1 - E_H) \quad (2)$$

$$E_H = 1 - CL_H/Q_H \quad (3)$$

where  $F$  represents the overall oral bioavailability,  $F_{abs}$  is the fraction of the oral dose absorbed intact across the apical membrane of the epithelial layer,  $E_G$  and  $E_H$  are the intestinal and hepatic extraction ratios, respectively,  $CL_H$  is the hepatic blood clearance and  $Q_H$  is the hepatic blood flow.

The bias of TDI prediction was assessed from the geometric mean of the ratio of predicted and actual value (average-fold error – *afe*, eq. 4). The mean squared prediction error (*mse*, eq 5) and the root mean squared prediction error (*rmse*, eq. 6) provided a measure of precision for the predictions of 37 in vivo TDIs assessing the contribution of  $k_{deg}$  and  $F_G$  ratio applying various inhibitor concentrations (Sheiner and Beal, 1981; Obach et al., 1997):



$$afe = 10^{\left| \frac{1}{n} \sum \log \frac{Predicted}{Observed} \right|} \quad (4)$$

$$mse = \frac{1}{n} \sum (Predicted - Observed)^2 \quad (5)$$

$$rmse = \sqrt{mse} \quad (6)$$

A 2-fold threshold value was selected on the basis of previous consensus reports (Tucker et al., 2001, Bjornsson et al., 2003) for a significant increase in AUC ratio. Thus predicted areas < 2 for interactions observed to be > 2 were classed as false negative and similarly, predicted areas > 2 for observed areas < 2 were classed as false positive interactions.

## Results

**In vivo data.** Previously reported time-dependent interactions (Table 1) have been classified using the recommendations of Bjornsson et al. (2003) for CYP3A4 inhibition interactions. Figure 1A shows the frequency distribution of the erythromycin, clarithromycin, azithromycin and diltiazem interactions observed in comparison to mibefradil, a well-known potent irreversible inhibitor of CYP3A4. This classification indicated that 54% of the interactions investigated were moderate (increase in AUC 2-5-fold), 14% were in the range of potent inhibition ( $AUC_i/AUC > 5$ ) and the remainder (32%) were weak ( $AUC_i/AUC < 2$ ).

**In vitro data.** TDI in vitro risk assessment is commonly based on the  $k_{inact}/K_I$  ratio as an indicator of in vitro potency. The  $k_{inact}$  values obtained for three macrolides and diltiazem ranged from 0.020-0.07  $\text{min}^{-1}$  (Table 2), resulting in a maximum inactivation  $t_{1/2}$  of 10-35 min for diltiazem and azithromycin, respectively, significantly longer than mibefradil (inactivation  $t_{1/2} = 1.7$  min) (Prueksaritanont et al., 1999). The  $k_{inact}/K_I$  ratio reported for N-desmethyldiltiazem (0.035) was equivalent to diltiazem. Literature reported estimates obtained in both human liver and recombinant enzymes show large variability (0.001-0.008 and 0.005-0.023, respectively in the case of erythromycin), with a general trend of greater estimated potency using recombinant enzymes in comparison to the liver microsomes. However, no direct relationship between the in vitro potency parameter and in vivo  $AUC_i/AUC$  ratios was observed as shown in Fig. 1B for eight time-dependent inhibitors, namely azithromycin, clarithromycin, erythromycin, diltiazem, verapamil, mibefradil, saquinavir and ritonavir. These findings are only partially dose-related as the same dose of erythromycin (1500 mg/day) results in either no effect (carbamazepine) or a 6-fold increase in AUC ratio (simvastatin) confirming that the in vitro parameters, although good indicators of potency, are not sufficient to predict the extent of TDI; additional substrate and inhibitor-related parameters are required.

**Impact of Enzyme Degradation and Parallel Elimination Pathways on TDI Prediction.** Human  $k_{deg}$  estimates from induction studies with carbamazepine or ritonavir are shown in Table 3. The small number of livers and the 7-fold range in CYP3A4  $t_{1/2deg}$  observed

represent a limitation of these estimates. The mean value of 3 days (corresponding to a  $k_{deg} = 0.00016 \text{ min}^{-1}$ ) is consistent with in vitro findings in liver slices (Renwick et al., 2000) and was applied in all our TDI predictions.

The simulation in Fig. 2 shows the combined effect of substrate-related ( $f_{m_{CYP3A4}} = 0.4-1$ ) and enzyme-related ( $k_{deg} = 0.00008 - 0.0005 \text{ min}^{-1}$ ) parameters on the predicted AUC ratio taking erythromycin as an example ( $k_{inact}$  and  $K_I$  values of  $0.025 \text{ min}^{-1}$  and  $13 \mu\text{M}$ , respectively for an  $[I]$  of  $0.5 \mu\text{M}$ , assuming no inhibition of the parallel pathway). The weak interaction potential predicted (2-fold increase in the AUC) refers to the substrates with low CYP3A4 contribution to the overall elimination (e.g., cerivastatin) in patients with a short CYP3A4  $t_{1/2deg}$ , whereas the compounds with  $f_{m_{CYP3A4}} > 0.9$  in patients with CYP3A4  $t_{1/2deg} = 6$  days represent the highest interaction risk (AUC increase up to 7-fold). The sensitivity of the predicted AUC ratios to different  $k_{deg}$  at high and low  $f_{m_{CYP3A4}}$  (0.9 and 0.5, respectively) over a range of inhibitor concentrations is illustrated in Fig. 3A and B for a weak and potent time-dependent inhibitor (e.g., azithromycin and mibefradil, respectively). Different CYP3A4  $t_{1/2deg}$  estimates have the greatest impact at higher  $f_{m_{CYP3A4}}$  values, a trend observed regardless of the inhibitor potency; the major difference is the inhibitor concentration required to achieve the maximum effect.

The effect of various  $k_{deg}$  (CYP3A4  $t_{1/2deg} = 1-6$  days), on the prediction accuracy of 15 erythromycin, 6 clarithromycin, 3 azithromycin and 13 diltiazem studies was investigated. Comparison of the predicted and observed  $AUC_i/AUC$  for 37 TDI studies using the mean  $k_{deg}$  value of  $0.00016 \text{ min}^{-1}$  (CYP3A4  $t_{1/2deg} = 3$  days),  $[I]_{av,u}$  and the corresponding  $f_{m_{CYP3A4}}$  is shown in Fig. 4A. Out of 37 studies, 89% were predicted within 2-fold of in vivo value; the use of extreme values (1 and 6 days) resulted in 22 and 25% of the studies under- or over-predicted, respectively. The prediction precision using the mean  $k_{deg}$  was improved by 10 and 21-fold (lower rmse) in comparison to the CYP3A4  $t_{1/2deg}$  of 1 and 6 days, respectively. In comparison to  $[I]_{av,u}$ , the use of  $[I]_{in,u}$  resulted in an increased number of over-predictions (up

to 41% for  $t_{1/2 \text{ deg}}$  of 6 days) and a generally lower prediction accuracy as 59-68 % of studies predicted were within 2-fold limits over the range of  $k_{\text{deg}}$ .

In all the scenarios investigated the contribution of N-desmethyldiltiazem, an equipotent time-dependent inhibitor to diltiazem, was incorporated in the prediction. The mechanism of inhibition is the same for both parent and metabolite and therefore the maximal inhibition effect is not significantly increased by incorporating the metabolite in the prediction. The net effect is  $f_{\text{mCYP3A4}}$ -dependent and decreases progressively with the decreasing contribution of CYP3A4 to the overall elimination of a substrate (from 19 to 0.5% for  $f_{\text{mCYP3A4}}=0.9$  and 0.1, respectively). A simulated interaction scenario with two inhibitors acting by the same mechanism where the second inhibitor is either equipotent (e.g., N-desmethyldiltiazem) or 5, 10 and 50-fold more potent (greater  $k_{\text{inact}}/K_i$  ratio) than the first inhibitor (erythromycin used as an example) is shown in Fig. 5 for the case when  $f_{\text{mCYP3A4}}$  is 0.9. The increased potency of the second inhibitor causes the maximal effect to be achieved at lower inhibitor concentrations, the level of which is dependent on the contribution of CYP3A4 to the elimination.

**Misspecification of the Inhibition Mechanism.** Prediction of TDI using the  $[I]/K_i$  approach with the assumption of reversible inhibition resulted in 70% of predictions being classified as false negatives and only 30% within 2-fold range of in vivo values (Table 4). In comparison, predictions made using the time-dependent model resulted in a marked reduction in false negatives and in a significant increase in the number of studies predicted within 2-fold (89% when no corrections for the intestinal interaction was incorporated) and up to 10-fold greater accumulation in the presence of macrolides/diltiazem, which corresponded well with the clinical observations.

**Maximal Intestinal Inhibition.** In order to assess the contribution of the gut wall to the interaction, the ratio of the intestinal wall availability in the presence and absence of the inhibitor ( $F_G'$  and  $F_G$ , respectively) is incorporated in the prediction equation based on hepatic estimates. Figure 6 shows the general relationship between  $F_G'/F_G$  ratio and the relative change in the intestinal clearance caused by an inhibitor (defined by the inactivation index -

$k_{\text{inact}} \cdot I/k_{\text{deg}} \cdot (K_I + I)$ ). For the case when this inactivation index is  $>1$  (resulting in more than 50% decrease in the intestinal clearance) the effect of  $F_G$  ratio is most pronounced for compounds with high intestinal extraction (e.g., buspirone, tacrolimus), whereas it is minimal for the drugs with intestinal extraction of around and below 50% (e.g., indinavir, alprazolam). The list of the  $F_G$  values collated from iv and oral studies for nine CYP3A4 substrates analyzed in the current study is presented in Table 5. For the remaining substrates (loratadine, cerivastatin, nitrazepam, terfenadine, carbamazepine, pimozide, cisapride and lovastatin, representing 24% of the interactions investigated)  $F_G$  values were not available and only hepatic inhibition was taken into consideration ( $F_G'/F_G$  assumed to be 1).

The  $F_G'/F_G$  ratio can be determined experimentally from the relative change in the intestinal clearance of a compound in the presence of an inhibitor. However, when this is not available, an initial estimate of the extent of intestinal inhibition can be obtained by assuming the 'worst case scenario', i.e., the maximum inhibition of intestinal CYP3A4 ( $F_G'=1$ ). Table 5 indicates a 5-fold range of maximum  $F_G'/F_G$  ratios for the nine CYP3A4 substrates investigated. An issue of concern is the extent of inter-individual variability in the estimates of  $F_G$ , exemplified by a range of values for midazolam intestinal extraction (43-63%) (Ollkolla et al., 1996, Thummel et al., 1996). For the majority of TDI studies involving erythromycin and clarithromycin inclusion of the maximal  $F_G'/F_G$  ratios improved the prediction; in contrast to the diltiazem studies which were mainly over-predicted. In addition, not surprisingly this correction was not advantageous to the minimal interactions observed with azithromycin.

Overall, the inclusion of the maximal  $F_G'/F_G$  ratio for the respective substrates increased the number of over-predictions and reduced the prediction accuracy (70% estimates were within 2-fold of in vivo value using the mean  $k_{\text{deg}}$ ) (Fig. 4B, Table 4). The number of over-predictions was related to the CYP3A4  $t_{1/2\text{deg}}$  used, increasing from 0 to 6 and from 9 to 16 for the  $t_{1/2\text{deg}}$  of 1-6 days, respectively. When  $[I]_{\text{in,u}}$  rather than  $[I]_{\text{av,u}}$  was applied in the prediction, the inclusion of the maximal  $F_G$  ratio resulted in the over-prediction of more than 50% of the studies, irrespective of the CYP3A4  $t_{1/2\text{deg}}$  used.

In addition to inhibitors the predictions of 28 TDI (using eq. 1, CYP3A4  $t_{1/2deg} = 3$  days, corresponding  $f_{mCYP3A4}$  and  $[I]_{av,u}$ ) before and after the  $F_G$  ratio correction (Fig. 4 C and D, respectively) are identified according to the particular substrates. In contrast to midazolam, triazolam and nifedipine interactions, which were generally improved by the gut correction, pronounced over-predictions were observed for the interactions with cyclosporine and buspirone, in particular with diltiazem as an inhibitor. In contrast to  $F_G = 1$ , the assumption that diltiazem reduces intestinal CYP3A4 activity by 62% (assessed by midazolam 1'-hydroxylation, Pinto et al., 2005), reduced this ratio and the extent of over-predictions mainly for cyclosporine and buspirone interactions by 54 to 190%, respectively; however, the predictions were still outside the 2-fold limits of in vivo values, in particular for cyclosporine.

## Discussion

The general approach to TDI in vitro risk assessment is based on the use of the  $k_{\text{inact}}/K_I$  ratio as an indicator of in vitro potency. However, there is a great variation in the methods used to generate this estimate, consistent with the 8-fold range observed in the literature reported estimates for erythromycin in human liver microsomes and recombinant enzymes. The large variability observed can only be partially related to the use of different in vitro probes to assess the remaining CYP3A4 activity (triazolam, midazolam or testosterone). Highly variable substrate concentrations used (e.g., midazolam at 8-200  $\mu\text{M}$ ) and differential methods applied for obtaining parameter estimates (linear or nonlinear regression analysis) observed here and in other studies (Ghanbari et al., submitted for publication) imply a need for a more consistent in vitro experimental design for quantitative TDI assessment. A recent correlation analysis of  $k_{\text{inact}}/K_I$  estimates for five HIV-protease inhibitors by Ernest et al. (2005) indicated higher potency estimates in recombinant enzymes in comparison to the liver microsomes, a trend also seen in the current analysis with macrolides. However, standardization of in vitro methodology and the use of the CYP3A4 probe at high substrate concentration (equivalent to the  $V_{\text{max}}$ ) in the study by Ernest et al. (2005) reduced the difference between the in vitro systems (with the exception of saquinavir) to only 2-fold. The extrapolation of the in vitro potency ( $k_{\text{inact}}/K_I$ ) to the in vivo situation depends on the relative magnitude of this parameter to the enzyme degradation; in the case when the inactivation index -  $k_{\text{inact}} \cdot I/k_{\text{deg}} \cdot (K_I + I)$  is  $\ll k_{\text{deg}}$  (<10%, e.g., azithromycin) a weak inhibitory effect can be expected, with the AUC ratio  $\leq 2$ . The opposite applies for moderate to potent inhibition; however, the relationship is more sensitive to the inhibitor concentration.

The current study investigated the impact of CYP3A  $t_{1/2\text{deg}}$  and the effect of maximal inhibition of intestinal metabolism (assessed by the  $F_G$  ratio) on the prediction of 37 TDI showing increases in AUC ratio of up to 7-fold. The substrates investigated cover a wide spectrum of interaction risk as they vary in the relative importance of CYP3A4 and renal clearance to their elimination, significance of intestinal first-pass, possible interplay with P-

glycoprotein (Benet et al., 2004) and contribution of CYP3A5 to the overall clearance (Galetin et al., 2004).

Venkatakrishnan and Obach (2005) have indicated the importance of accurate enzyme degradation estimates for the prediction of CYP2D6 inactivation by paroxetine; however there is no comparable study performed for CYP3A4. Most of the prediction work in the area of time-dependent interactions is based on the use of CYP3A4  $t_{1/2deg}$  estimates obtained in either rat or Caco-2 cells (Ito et al., 2003, Wang et al., 2004). A number of indirect methods (Table 3) have been used to assess the CYP3A4  $t_{1/2deg}$ , all showing a great extent of inter-individual variability. Therefore, the current study examines the impact of a range of human CYP3A4  $t_{1/2deg}$  (20-146 hrs used as the extreme values) on the assessment of TDI potential. The mean estimated decay of CYP3A4 activity is in general longer in comparison to most other cytochrome P450 enzymes (Ghanbari et al., submitted for publication). Differential degradation half-lives reported for CYP3A4 and CYP3A5 in vitro (79 vs. 35 hrs, respectively (Renwick et al., 2000)) and less susceptibility to inhibition observed for CYP3A5 (McConn et al., 2004) may contribute to the extent of inter-individual variability observed in the magnitude of interactions.

The effect of the CYP3A  $k_{deg}$  on the predicted AUC ratios for 37 interactions with macrolides and diltiazem was dependent on the inhibitor concentration used in the prediction. Use of the mean  $k_{deg}$  ( $0.00016 \text{ min}^{-1}$ ) and  $[I]_{av,u}$ , with no corrections for the intestinal interaction, provided low bias and the highest precision of TDI predictions (Table 4), with 33/37 studies predicted within 2-fold (Fig. 4A), whereas use of  $[I]_{in,u}$  was generally poorer. For all the scenarios investigated ( $t_{1/2deg} = 1-6$  days) the use of total inhibitor concentration, in particular hepatic input values, resulted in the significant over-prediction regardless of the CYP3A4  $t_{1/2deg}$  estimates used. As indicated previously for CYP2D6 (Venkatakrishnan and Obach, 2005), the sensitivity of the predicted extent of interaction to the differential CYP3A4 degradation rate was dependent on  $f_{mCYP3A4}$ , as illustrated in Figs. 2 and 3. The current analysis indicates the suitability of the mean CYP3A4  $t_{1/2deg}$  of 3 days in the assessment of time-dependent interaction potential.



For CYP3A4 substrates a certain degree of interaction at the level of the gut wall is to be expected as the small intestine represents the first in the series of the first pass eliminating organs and is exposed to the orally administered inhibitors or inducers. A number of studies indicated a more pronounced inhibition (and induction) of intestinal CYP3A4 in comparison to the liver (Floren et al., 1997, Gomez et al., 1995, Tsunoda et al., 1999). The interpretation of such events has to be cautious for compounds that are mutual substrates for P-glycoprotein and CYP3A4 (e.g., cyclosporine, tacrolimus) due to their interactive nature and differing inter-relationship in the intestine and liver (Benet et al., 2004). Intestinal interactions are rarely incorporated in the assessment of interaction potential, either for reversible or irreversible types (Rostami-Hodjegan and Tucker, 2004), which may represent a limitation for some CYP3A4 compounds. For example, a 2.6-fold greater increase in the  $AUC_i/AUC$  ratio after oral dose of midazolam in comparison to the iv administration was observed in the presence of clarithromycin, indicating the contribution of intestinal interaction (Gorski et al., 1998). This observed difference is in good agreement with the predicted maximal intestinal  $F_G$  ratio (Table 5). Predicted values of the maximal  $F_G'/F_G$  ratio are directly related to the accuracy of the initial estimates of the intestinal extraction and are based on the assumption that the extent of intestinal metabolism after iv administration is negligible and that absorption is complete, which may not be correct. The sensitivity of TDI prediction to the inter-individual variability observed in the estimates of  $F_G$  is greatest for substrates with  $F_G < 0.5$  (e.g., buspirone), as illustrated in Fig. 6.

The current study assessed the impact of assuming maximal intestinal inhibition ( $F_G'=1$ ) and despite the fact that some of the inhibitors investigated show moderate/weak potency this assumption was satisfactory. The highest concentrations of the inhibitor are expected during its absorption phase and the number of weak interactions (azithromycin being the weakest inhibitor investigated) is small in comparison to the overall number of studies. Out of 28 studies where the corrections for the intestinal interaction were applied, 18 were predicted within the 2-fold of in vivo value with a low number of false negative predictions. However, in 10 cases incorporation of the  $F_G$  ratio (notably for diltiazem studies) resulted in

an over-prediction (Fig. 4B and D). In addition to the inhibitor, this observed over-prediction trend can also be associated with the substrate-related characteristics as illustrated in Figs. 4C and D. The over-estimate of the magnitude of interaction observed in the case of cyclosporine is anticipated due to the possible contribution of efflux transporters and initial over-prediction of the significance of the intestinal metabolism. For this and other high permeability/low solubility compounds like tacrolimus and lovastatin (Wu and Benet, 2005) the relationship between the  $F_G$  ratio and the inhibitor potency will be more complex in comparison to the substrates mainly cleared by metabolism (e.g., midazolam, nifedipine). In the case of midazolam, maximal predicted and observed  $F_G$  ratios were in good agreement in the presence of a number of irreversible and reversible inhibitors (data not shown); however, the general lack of iv studies undertaken prevents a more comprehensive comparison.

Prediction of TDI using the  $[I]/K_i$  approach and the assumption of a reversible inhibition process generally results in the false negative predictions (Ito et al., 2004, Venkatakrishnan and Obach, 2005). When this model was employed for the prediction of interactions with macrolides and diltiazem, 70% of the studies investigated were under-predicted (by 2 to 7-fold), whereas the time-dependent prediction model described here decreased the percentage of false negatives to 19 and 8 % before and after the  $F_G$  ratio correction, respectively (Table 4).

In conclusion, the current study provides a systematic analysis of the impact of CYP3A4 degradation rate, parallel elimination pathways and intestinal inhibition on the prediction of a range of TDI. The impact of a differential CYP3A4 degradation rate on the prediction accuracy and precision is important for substrates where CYP3A4 contributes more than 50% to the overall elimination. Maximal  $F_G$  ratio is proved to be a useful initial indicator of the extent of intestinal inhibition and minimized the number of false negative predictions. However, the increased number of over-predictions observed for true positive TDI when the maximal intestinal inhibition was assumed indicated a need for further evaluation of this approach and assessment of the interplay with the efflux transporters and variability in  $F_G$  estimates.

### **Acknowledgement**

Authors are grateful to Dr Amin Rostami-Hodjegan (University of Sheffield and Simcyp Ltd) for useful discussions.

**References:**

Austin RP, Barton P, Cockroft SL, Wenlock MC and Riley RJ (2002) The influence of non-specific microsomal binding on apparent intrinsic clearance, and its prediction from physicochemical properties. *Drug Metab Dispos* **30**: 1497-1503.

Benet LZ, Cummins CL and Wu CY (2004) Unmasking the dynamic interplay between efflux transporters and metabolic enzymes. *Int J Pharmaceut* **277**: 3-9.

Bjornsson TD, Callaghan JT, Einolf HJ, Fischer V et al. (2003) The conduct of in vitro and in vivo drug-drug interaction studies: a pharmaceutical research and manufacturers of America (PhRMA) perspective. *Drug Metab Dispos* **31**: 815-832.

Brown HS, Ito K, Galetin A and Houston JB (2005) Prediction of in vivo drug-drug interactions from in vitro data: impact of incorporating parallel pathways of drug elimination and inhibitor absorption rate constant *Br J Clin Pharmacol* j.1365-2125.2005.02483.x

Correia MA (1991) Cytochrome P450 turnover. *Methods Enzymol* **206**: 315-325.

Echizen H and Eichelbaum M (1986) Clinical pharmacokinetics of verapamil, nifedipine and diltiazem. *Clin Pharmacokinet* **11**: 425-449.

Egnell A-C, Houston JB and Boyer S (2003) *In vivo* heteroactivation is a possible mechanism for the drug interaction between felbamate and carbamazepine cooperativity. *J Pharmacol Exp Ther* **305**: 1251-1262.

Ernest II CS, Hall SD and Jones DR (2005) Mechanism-based inactivation of CYP3A by HIV protease inhibitors. *J Pharmacol Exp Ther* **312**: 583-591.

Floren LC, Bekersky I, Benet LZ, Mekki Q, Dressler D, Lee JW, Roberts JP and Hebert MF (1997) Tacrolimus oral bioavailability doubles with coadministration of ketoconazole. *Clin Pharmacol Ther* **62**: 41-49.

Galetin A, Ito K, Hallifax D and Houston JB (2005) CYP3A4 substrate selection and substitution in the prediction of potential drug-drug interaction. *J Pharmacol Exp Ther* **314**:180-190.

Galetin A, Brown C, Hallifax D, Ito K and Houston JB (2004) Utility of recombinant enzyme kinetics in prediction of human clearance – impact of variability, CYP3A5 and CYP2C19 on CYP3A4 substrates *Drug Metab Dispos* **32**: 1411-1420.

Ghanbari F, Rowland-Yeo K, Bloomer J, Clarke S, Lennard MS, Tucker GT and Rostami-Hodjegan A A critical evaluation of the experimental design of studies of mechanism based inhibition, with implications for in vitro-in vivo extrapolation (submitted for publication)

Gomez DY, Wachter VJ, Tomlanovich SJ, Hebert MF and Benet LZ (1995) The effects of ketoconazole on the intestinal metabolism and bioavailability of cyclosporine. *Clin Pharmacol Ther* **58**: 15-19.

Gorski JC, Jones DR, Haehner-Daniels BD, Hamman MA, O'Mara EM Jr and Hall SD (1998) The contribution of intestinal and hepatic CYP3A to the interaction between midazolam and clarithromycin. *Clin Pharmacol Ther* **64**: 133-143.

Hall SD, Thummel KE, Watkins PB, Lown KS, Benet LZ, Paine MF, Mayo RR, Turgeon DK, Bailey DG, Fontana RJ and Wrighton SA (1999) Molecular and physical mechanisms of first-pass extraction. *Drug Metab Dispos* **27**: 161-166.

Hsu A, Granneman GR, Witt G, Locke C, Denissen J, Molla A, Valdes J, Smith J, Erdman K, Lyons N, Niu P, Decourt J-P, Fourtillan J-P, Girault J and Leonard JM (1997) Multiple-dose pharmacokinetics of ritonavir in human immunodeficiency virus-infected subjects. *Antimicrob Agents Chemother* **41**: 898-905.

Ito K, Hallifax D, Obach S and Houston JB (2005) Impact of parallel pathways of drug elimination and multiple cytochrome P450 involvement on drug-drug interactions: CYP2D6 paradigm. *Drug Metab Dispos* **33**: 837-844.

Ito K, Brown HS and Houston JB (2004) Database analyses for the prediction of in vivo drug-drug interactions from in vitro data. *Br J Clin Pharmacol* **57**: 473-486 and Erratum *Br J Clin Pharmacol* **58**: 565-568.

Ito K, Ogihara K, Kanamitsu S-I and Itoh T (2003) Prediction of the in vivo interaction between midazolam and macrolides based on in vitro studies using human liver microsomes. *Drug Metab Dispos* **31**: 945-954.

Kent UM, Jushchyshyn MI and Hollenberg PF (2001) Mechanism-based inactivators as probes of cytochrome P450 structure and function. *Curr Drug Metab* **2**: 215-243.

Lai AA, Levy RH and Cutler RE (1978) Time-course of interaction between carbamazepine and clonazepam in normal man. *Clin Pharmacol Ther* **24**: 316-323.

Malhotra S, Schmiedlin-Ren P, Paine MF, Criss AB and Watkins P (2001) The furocoumarin 6',7'-dihydroxybergamottin (DHB) accelerates CYP3A4 degradation via the ubiquitin-proteasomal pathway. *Drug Metab Rev* **33**: 97.

Mayhew BS, Jones DR and Hall SD (2000) An in vitro model for predicting in vivo inhibition of cytochrome P450 3A4 by metabolic intermediate complex formation *Drug Metab Dispos* **28**: 1031-1037.

McConn DJ II, Lin YS, Alen K, Kunze KL, Thummel KE (2004) Differences in the inhibition of cytochromes P450 3A4 and 3A5 by metabolite-inhibitor complex-forming drugs. *Drug Metab Dispos* **32**: 1083-1091.

Obach RS, Baxter JG, Liston TE, Silber BM, Jones BC, MacIntyre F, Rance DJ and Wastall P (1997) The prediction of human pharmacokinetic parameters from preclinical and in vitro metabolism data. *J Pharmacol Exp Ther* **283**: 46-58.

Olkkola KT, Ahonen J and Neuvonen PJ (1996) The effects of the systemic antimycotics, itraconazole and fluconazole, on the pharmacokinetics and pharmacodynamics of intravenous and oral midazolam. *Anesth Analg* **82**:511-516.

Pinto AG, Horlander J, Chalasani N, Hamman M, Asghar A, Kolwankar D and Hall SD (2005) Diltiazem inhibits human intestinal cytochrome P450 3A (CYP3A) activity in vivo without altering the expression of intestinal mRNA or protein. *Br J Clin Pharmacol* **59**: 440-446.

Prueksaritanont T, Ma B, Tang C, Meng Y, Assang C, Lu P, Reider PJ, Lin JH and Baillie TA (1999) Metabolic interactions between mibefradil and HMG-CoA reductase inhibitors: an in vitro investigation with human liver microsomes. *Br J Clin Pharmacol* **47**: 291-298.

Renwick AB, Watts PS, Edwards RJ, Barton PT, Guyonnet I, Price RJ, Tredger M, Pelkonen O, Boobis A and Lake BG (2000) Differential maintenance of cytochrome P450 enzymes in cultured precision-cut liver slices. *Drug Metab Dispos* **28**: 1202-1209.

Rostami-Hodjegan A and Tucker GT (2004) 'In silico' simulations to assess the 'in vivo' consequences of 'in vitro' metabolic drug-drug interactions. *Drug Discovery Today: Technologies* **1**: 441-448.

Rowland Yeo K and Yeo WW (2001) Inhibitory effects of verapamil and diltiazem on simvastatin metabolism in human liver microsomes. *Br J Clin Pharmacol* **51**: 461-470.

Sheiner LB and Beal SL (1981) Some suggestions for measuring predictive performance. *J Pharmacokinetic Biopharm* **9**: 503-512.

Silverman RB (1995) Mechanism-based inactivators. *Methods Enzymol* **249**: 240-283.

Thummel KE, O'Shea D, Paine MF, Shen DD, Kunze KL, Perkins JD and Wilkinson GR (1996) Oral first-pass elimination of midazolam involves both gastrointestinal and hepatic CYP3A-mediated metabolism. *Clin Pharmacol Ther* **59**: 491-502.

Tsunoda SM, Velez RL, von Moltke LL and Greenblatt DJ (1999) Differentiation of intestinal and hepatic cytochrome P450 3A activity with use of midazolam as an in vivo probe: the effect of ketoconazole. *Clin Pharmacol Ther* **66**: 461-471.

Tucker GT, Houston JB and Huang, S-M (2001) Optimizing drug development: Strategies to assess drug metabolism/transporter interaction potential - toward a consensus. *Clin Pharmacol Ther* **70**: 103-114.

Venkatakrishnan and Obach (2005) In vitro-in vivo extrapolation of CYP2D6 inactivation by paroxetine: prediction of non-stationary pharmacokinetics and drug interaction magnitude. *Drug Metab Dispos* **33**: 845-852.



Wang R, Fu Y and Lai L (1997) A new atom-additive method for calculating partition coefficients. *J Chem Inf Comp Sci* **37**:615-621.

Wang Y-H, Jones DR and Hall SD (2004) Prediction of cytochrome P450 3A inhibition by verapamil enantiomers and their metabolites. *Drug Metab Dispos* **32**: 259-266.

Wu C-Y and Benet LZ (2005) Predicting drug disposition via application of BCS: Transport/absorption/elimination interplay and development of a biopharmaceutics drug disposition classification system. *Pharm Res* **22**: 11-23.

Zhou S, Chai SY, Goh BC, Chan E, Duan W, Huang M and McLeod HL (2005) Mechanism-based inhibition of cytochrome P450 3A4 by therapeutic drugs. *Clin Pharmacokinet* **44**: 279-304.

## **FOOTNOTES**

Financial support for this project was provided by the following Centre for Applied Pharmacokinetic Research Consortium members: Eli Lilly, GlaxoSmithKline, Novartis, Pfizer and Servier.

### **Address correspondence to:**

Dr A. Galetin, School of Pharmacy and Pharmaceutical Sciences, University of Manchester, Oxford Rd, Manchester, M13 9PL, UK

## Figure Legends

**Fig. 1. Assessment of inhibitory potential of macrolides, diltiazem and other compounds in vivo and in vitro.** **A**, Classification of azithromycin, erythromycin, clarithromycin, diltiazem and mibefradil interactions according to Bjornsson et al. (2003) where  $AUC_i/AUC > 5$  indicate potent,  $2 < AUC_i/AUC < 5$  moderate and  $AUC_i/AUC < 2$  weak interactions. **B**, Relationship between obtained  $k_{inact}/K_I$  ratio and the degree of interaction observed in vivo for azithromycin (1), erythromycin (2), clarithromycin (3), diltiazem (4), verapamil (5), mibefradil (6), saquinavir (7) and ritonavir (8) (inhibitors are listed in the order of increasing  $k_{inact}/K_I$ ).

**Fig. 2. Effect of  $fm_{CYP3A4}$  and CYP3A4  $t_{1/2deg}$  on the predicted AUC ratio.** Surface simulated for erythromycin  $k_{inact}$  and  $K_I$  values ( $0.025 \text{ min}^{-1}$  and  $13 \text{ } \mu\text{M}$ , respectively) for inhibitor concentration of  $0.5 \text{ } \mu\text{M}$  over the range of  $fm_{CYP3A4} = 0.4-1$  and CYP3A4  $t_{1/2deg} = 1-6$  days; eq. 1 was used with  $F_G'/F_G = 1$ .

**Fig. 3. Effect of CYP3A4 degradation half-life on AUC ratio for inhibitors with different potency.** The sensitivity of the predicted AUC ratios on  $t_{1/2deg}$  of 1 (---), 3 (—) and 6 days (—) at high and low  $fm_{CYP3A4}$  (0.9 and 0.5, respectively) over a range of inhibitor concentrations for azithromycin (A) and mibefradil (B); eq. 1 was used with  $F_G'/F_G = 1$ .

**Fig. 4. Relationship between predicted and observed AUC ratios for time-dependent interactions.** **A**, Prediction of 37 TDI using eq. 1 applying the average unbound plasma concentration of the inhibitor, corresponding  $fm_{CYP3A4}$  and CYP3A4  $t_{1/2deg}$  of 3 days ( $F_G$  ratio = 1). Interactions identified according to the inhibitors: ■ represents azithromycin (3), △ erythromycin (15), ● clarithromycin (6) and \* diltiazem (13). **B**, Effect of incorporating the maximal intestinal inhibition ( $F_G' = 1$ ) on the prediction; all other conditions and symbols are as in panel A.

**C**, Predictions of 28 TDI using eq. 1 (CYP3A4  $t_{1/2deg}$ ,  $fm_{CYP3A4}$  and  $[I]_{av,u}$  as in panel A) using the nine substrates with the available  $F_G$  value. Interactions identified according to the substrates:  $\triangle$  represents midazolam,  $\circ$  triazolam,  $\square$  alprazolam,  $\blacktriangle$  buspirone,  $\blacktriangledown$  quinidine,  $\diamond$  simvastatin,  $\blacksquare$  cyclosporine,  $\bullet$  felodipine and  $*$  nifedipine. **D**, Effect of incorporating the maximal intestinal inhibition ( $F_G = 1$ ) on the predictions; all other conditions and symbols are as in panel C.

In all the panels the solid line represents line of unity, whereas dashed lines represent the 2-fold limit in prediction accuracy. The shaded areas correspond to the true negative and positive time-dependent interactions defined by the 2-fold increase in the AUC.

**Fig. 5. Simulations of interactions with multiple time-dependent inhibitors.** The mechanism of inhibition is assumed to be the same and the second inhibitor is either equipotent or 5, 10 and 50-fold more potent (greater  $k_{inact}/K_I$  ratio) than the first inhibitor for the case when  $fm_{CYP3A4}$  is 0.9; eq. 1 was used with  $F_G'/F_G = 1$ .

**Fig. 6.** Relationship between  $F_G'/F_G$  and inactivation index -  $k_{inact} \cdot I/k_{deg} \cdot (K_I + I)$  for varying degrees of intestinal extraction (0-1).  $F_G'/F_G$  was simulated from the relative change in the intestinal intrinsic clearance caused by the inhibitor which is estimated from the inactivation index parameters (Wang et al., 2004).

TABLE 1

*Observed in vivo AUC<sub>i</sub>/AUC ratios for 37 CYP3A4 time-dependent interactions*

	<b>Interaction</b>	<b>Mean AUC<sub>i</sub>/AUC</b>	<b>fm<sub>CYP3A4</sub></b>	<b>Reference</b>
	<b>Erythromycin</b>			
1	+ Alprazolam	2.5	0.8	Yasui et al. (1996) <i>Clin Pharmacol Ther</i> <b>59</b> : 514-519.
2	+ Buspirone	5.9	0.99	Kivisto et al. (1997) <i>Clin Pharmacol Ther</i> <b>62</b> : 348-354.
3	+ Carbamazepine	1.4	0.6	Barzaghi et al. (1987) <i>Br J Clin Pharmacol</i> 1987; <b>24</b> : 836-38.
4	+ Cerivastatin	1.21	0.37	Muck et al. (1998) <i>Eur J Clin Pharmacol</i> <b>53</b> : 469-473.
5	+ Cyclosporine*	2.15	0.71	Gupta et al. (1989) <i>Br J Clin Pharmacol</i> <b>27</b> : 475-481.
6	+ Cyclosporine*	2.22	0.71	Freeman et al. (1987) <i>Br J Clin Pharmacol</i> <b>23</b> : 776-778.
7	+ Felodipine	2.5	0.81	Bailey et al. (1996) <i>Clin Pharmacol Ther</i> <b>60</b> : 25-33.
8	+ Loratadine	1.5	0.6	Brannan et al. (1995) <i>Clin Pharmacol Ther</i> <b>58</b> : 269-278.
9	+ Midazolam	4.11	0.94	Zimmermann et al. (1996) <i>Arzneimittelforschung</i> <b>46</b> : 213-217 and Olkkola et al. (1993) <i>Clin Pharmacol Ther</i> <b>53</b> : 298-305.
10	+ Nitrazepam	1.25	0.6	Luurila et al. (1995) <i>Pharmacol Toxicol</i> <b>76</b> : 255-258.
11	+ Quinidine	1.2	0.76	Damkier et al. (1999) <i>Br J Clin Pharmacol</i> <b>48</b> : 829-838.
12	+ Simvastatin	6.2	0.99	Kantola et al. (1998) <i>Clin Pharmacol Ther</i> <b>64</b> : 177-182.
13	+ Terfenadine	2.1	0.74	Honig et al. (1994) <i>Drug Invest</i> <b>7</b> : 148-156.
14	+ Triazolam	2.06	0.92	Phillips et al. (1986) <i>J Clin Psychopharmacol</i> <b>6</b> : 297-299.
15	+ Triazolam	3.36	0.92	Greenblatt et al. (1998) <i>Clin Pharmacol Ther</i> <b>64</b> : 278-285.

<b>Clarithromycin</b>				
16	+ Cisapride	3.16	0.95	van Haarst et al. (1998) <i>Clin Pharmacol Ther</i> <b>64</b> : 542-546.
17	+ Midazolam	3.6	0.94	Yeates et al. (1996) <i>Int J Clin Pharmacol Ther</i> <b>34</b> :400-405.
18	+ Midazolam	7	0.94	Gorski et al. (1998) <i>Clin Pharmacol Ther</i> <b>64</b> : 133-143.
19	+ Pimozide	2.12	0.4	Desto et al. (1999) <i>Clin Pharmacol Ther</i> <b>65</b> : 10-20.
20	+ Terfenadine	2.5	0.74	Honig et al. (1994) <i>Drug Invest</i> <b>7</b> :148-156.
21	+ Triazolam	5.1	0.92	Greenblatt et al. (1998) <i>Clin Pharmacol Ther</i> <b>64</b> : 278-285.
<b>Azithromycin</b>				
22	+ Midazolam	0.87	0.94	Backman et al. (1995) <i>Int J Clin Pharmacol Ther</i> <b>33</b> : 356-359.
23	+ Midazolam	1.23	0.94	Zimmermann et al. (1996) <i>Arzneimittelforschung</i> <b>46</b> : 213-217.
24	+ Triazolam	1.03	0.92	Greenblatt et al. (1998) <i>Clin Pharmacol Ther</i> <b>64</b> : 278-285.
<b>Diltiazem</b>				
25	+ Cyclosporine*	1.49	0.71	Asberg et al. (1999) <i>Eur J Clin Pharmacol</i> <b>55</b> : 383-387.
26	+ Cyclosporine*	1.57	0.71	Foradoti et al. (1998) <i>Transplat Proc</i> <b>30</b> : 1685-1687.
27	+ Cyclosporine*	1.25	0.71	Brockmoller et al. (1990) <i>Eur J Clin Pharmacol</i> <b>38</b> : 237-242.
28	+ Lovastatin	3.6	0.99	Azie et al. (1998) <i>Clin Pharmacol Ther</i> <b>64</b> : 369-377.
29	+ Midazolam	3.75	0.94	Backman et al. (1994) <i>Br J Clin Pharmacol</i> <b>37</b> : 221-225.
30	+ Nifedipine	2.22	0.71	Tateishi et al. (1989) <i>J Clin Pharmacol</i> <b>29</b> : 994-997.
31	+ Nifedipine	3.11	0.71	Tateishi et al. (1989) <i>J Clin Pharmacol</i> <b>29</b> : 994-997.
32	+ Nifedipine	2.39	0.71	Ohashi et al. (1990) <i>J Cardiovasc Pharmacol</i> <b>15</b> : 96-101.
33	+ Simvastatin	4.82	0.99	Mousa et al. (2000) <i>Clin Pharmacol Ther</i> <b>67</b> : 267-274.

34	+ Triazolam	3.38	0.92	Varhe et al. (1996) <i>Clin Pharmacol Ther</i> <b>59</b> : 369-375.
35	+ Triazolam	2.3	0.92	Kosuge et al. (1997) <i>Br J Clin Pharmacol</i> <b>43</b> : 367-372.
36	+ Buspirone	5.5	0.99	Lamberg et al. (1998) <i>Clin Pharmacol Ther</i> <b>63</b> : 640-645.
37	+ Quinidine	1.53	0.76	Laganiere et al. (1996) <i>Clin Pharmacol Ther</i> <b>60</b> : 255-264.

\* $f_{m_{CYP3A4}}$  values obtained by regression analysis using eq. 1

TABLE 2

*List of inhibitor concentrations and in vitro estimates for macrolides and diltiazem used for the prediction of 37 time-dependent interactions*

	$[I]_{av,u}$ ( $\mu\text{M}$ ) <sup>a</sup>	$[I]_{in,u}$ ( $\mu\text{M}$ ) <sup>a</sup>	$k_{inact}$ ( $\text{min}^{-1}$ )	$K_I$ ( $\mu\text{M}$ )	Reference (in vitro data)
<b>Azithromycin<sup>b</sup></b>	0.1 – 0.2	0.31 – 0.63	0.02	656	Ito et al., 2003
<b>Erythromycin<sup>b</sup></b>	0.08 – 0.17	0.3 – 0.6	0.025	13.35	Ito et al., 2003
<b>Clarithromycin<sup>b</sup></b>	0.14 – 0.28	1.2 – 2.4	0.044	39	Ito et al., 2003
<b>Diltiazem<sup>c,d</sup></b>	0.02 – 0.05	0.33 – 1.3	0.07	2	Rowland Yeo and Yeo, 2001

<sup>a</sup> The unbound fractions to the plasma protein were 0.16, 0.7, 0.28 and 0.175 for erythromycin, clarithromycin, azithromycin and diltiazem, respectively. Same plasma protein binding as for diltiazem and the relative plasma concentration of 38% of the parent were assumed for N-desmethyldiltiazem (Echizen and Eichelbaum, 1986).

<sup>b</sup> The values represent the mean of estimates obtained for two midazolam pathways (1'- and 4-hydroxy).

<sup>c</sup>  $K_I$  value corrected for the microsomal fraction unbound of 0.61 as described in Methods.

<sup>d</sup> The  $k_{inact}$  and  $K_I$  for N-desmethyldiltiazem were 0.027 and 0.77, respectively (Mayhew et al., 2000).



TABLE 3

*CYP3A4 degradation rate constant and the corresponding half-lives in human*

<b>k<sub>deg</sub> (min<sup>-1</sup>)</b>	<b>t<sub>1/2deg</sub> (hrs)</b>	
	<b>Mean (range)</b>	<b>Method and Reference</b>
0.00016	72	
0.00008- 0.0005	20-146 (n=7)	Carbamazepine induction; Lai et al. (1978)
0.00014	85 ± 61 (n=16)	Ritonavir autoinduction; Hsu et al. (1997)
0.00023 – 0.00032	36 – 50 (n=8)	Rifampin induction; Fromm et al. (1996)
	79	
0.00015	(17-no decay) (n=4)	In vitro data; Renwick et al. (2000)

TABLE 4

*Comparison of predictions applying reversible and time-dependent inhibition mechanism (with or without the correction for the intestinal interaction)*

<b>Number of studies</b>	<b>Reversible mechanism</b>	<b>Time-dependent mechanism</b>	<b>Time-dependent mechanism with <math>F_G'/F_G</math></b>
<b>False negative</b>	26	7	3
<b>False positive</b>	0	4	4
<b>Within 2-fold of in vivo</b>	11	33	26
<b>Over-predicted</b>	0	2	11
<b>afe</b>	2.4	1	1.6
<b>rmse</b>	11	0.47	15

TABLE 5

List of  $F_G$  values and the maximum  $F_G$  ratio values for nine CYP3A4 substrates investigated. Complete intestinal inhibition is assumed ( $F_G'=1$ )

CYP3A Substrate	$F_G$	Maximum $F_G'/F_G$	Reference
Buspirone	0.21	4.76	Obach RS, Walsky RL, Venkatakrishnan K, Gaman EA, Houston JB and Tremaine LM (submitted for publication)
Cyclosporine	0.39	2.6	Hebert et al. (1992) <i>Clin Pharmacol Ther</i> <b>52</b> : 453-455.
Felodipine	0.45	2.2	Lundahl et al. (1997) <i>Eur J Clin Pharmacol</i> <b>52</b> : 139-145.
Midazolam	0.57	1.75	Thummel et al. (1996) <i>Clin Pharmacol Ther</i> <b>59</b> : 491-502.
Triazolam	0.6	1.67	Masica et al. (2004) <i>Clin Pharmacol Ther</i> <b>76</b> : 341-349.
Simvastatin	0.66	1.51	Obach RS, Walsky RL, Venkatakrishnan K, Gaman EA, Houston JB and Tremaine LM (submitted for publication)
Nifedipine	0.74	1.35	Holtbecker et al. (1996) <i>Drug Metab Dispos</i> <b>24</b> : 1121-1123.
Quinidine	0.9	1.11	Damkier et al. (1999) <i>Eur J Clin Pharmacol</i> <b>55</b> : 451-456.
Alprazolam	0.98	1.02	Hirota et al. (2001) <i>Biopharm Drug Dispos</i> <b>22</b> : 53-71.

Figure 1

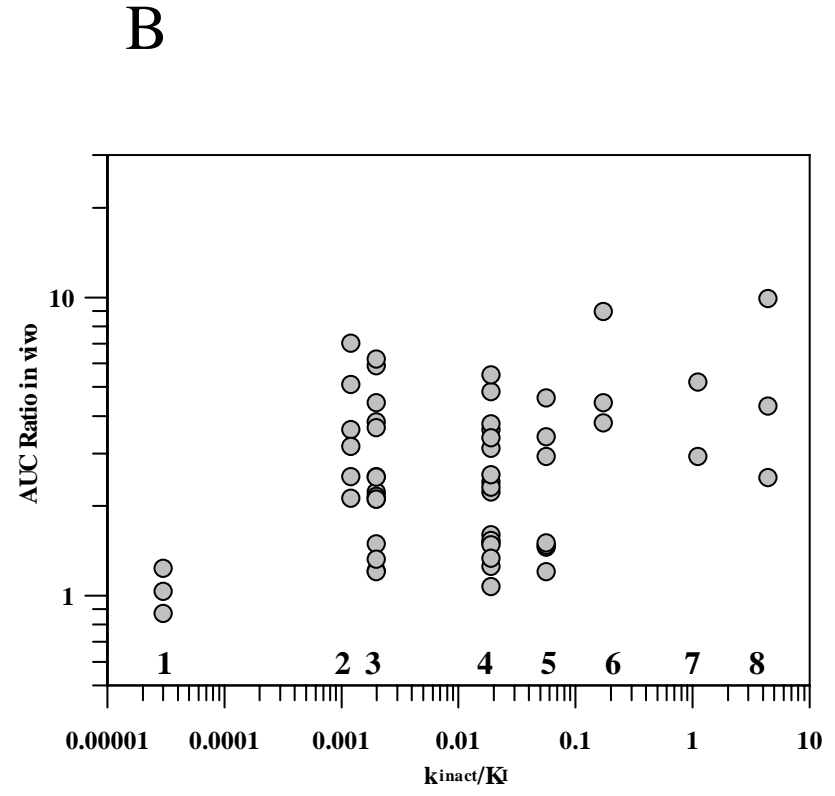
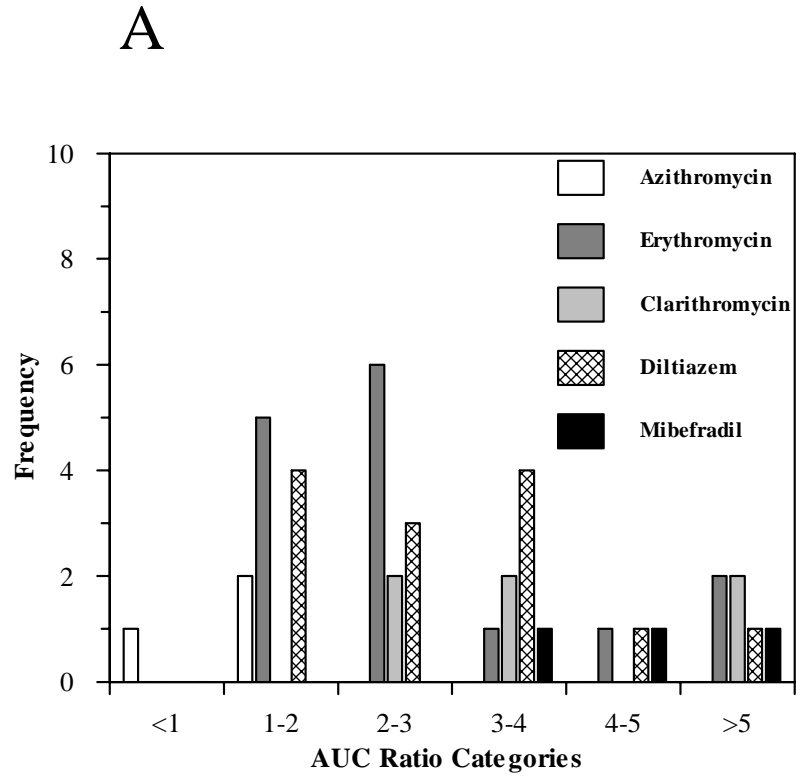


Figure 2

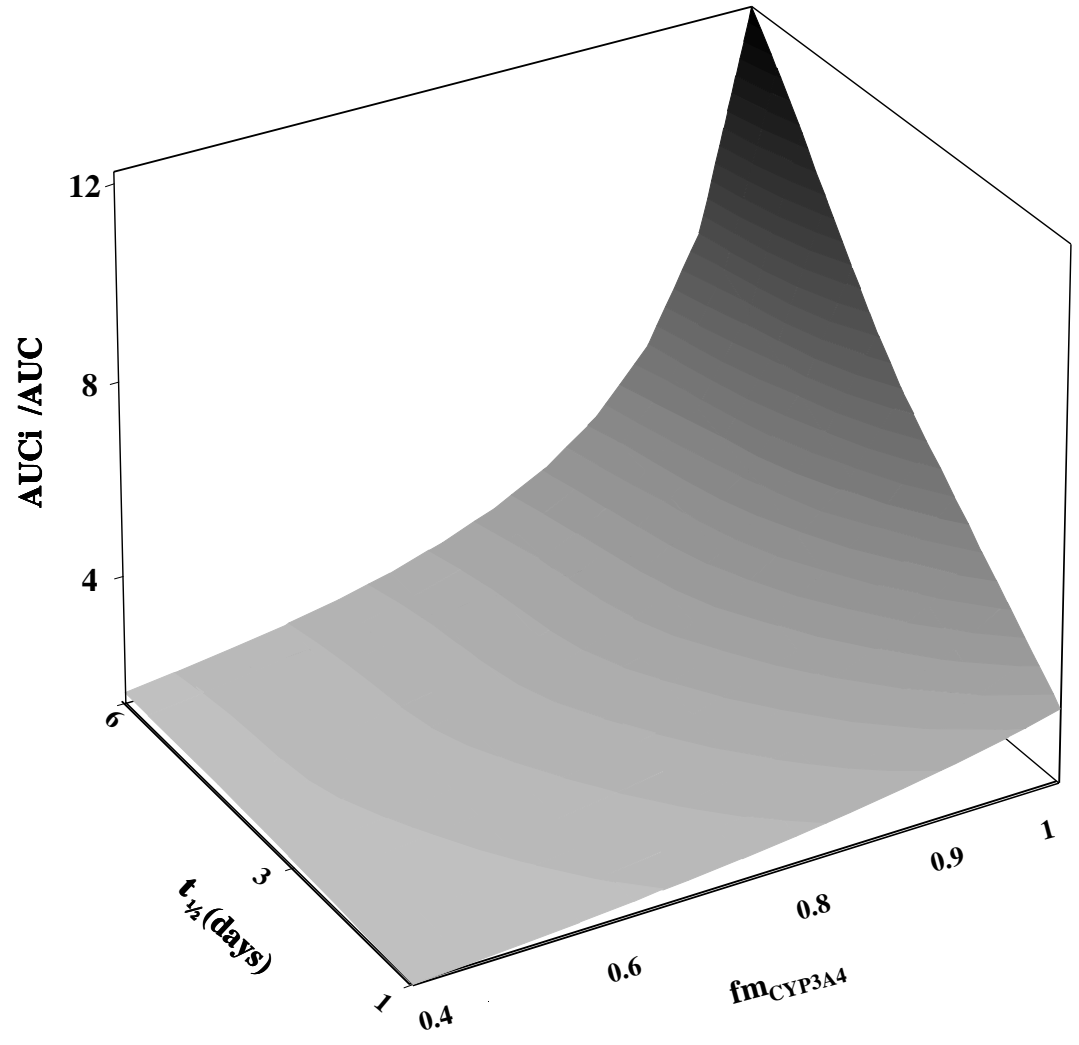
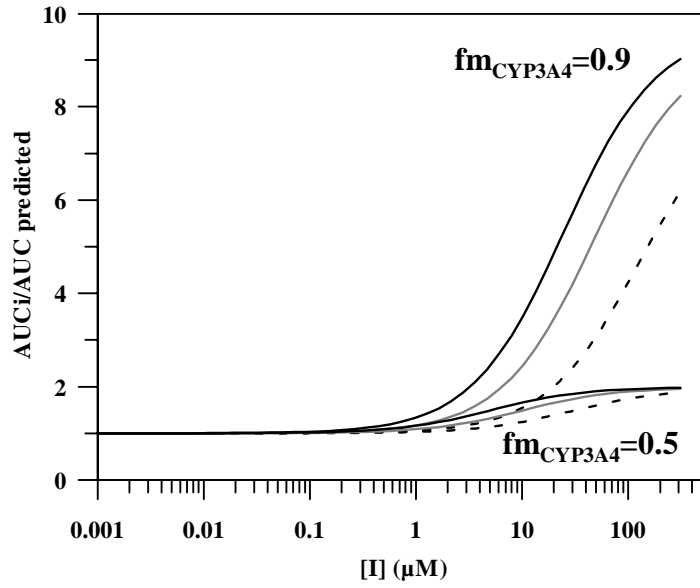


Figure 3

A - Azithromycin



B - Mibefradil

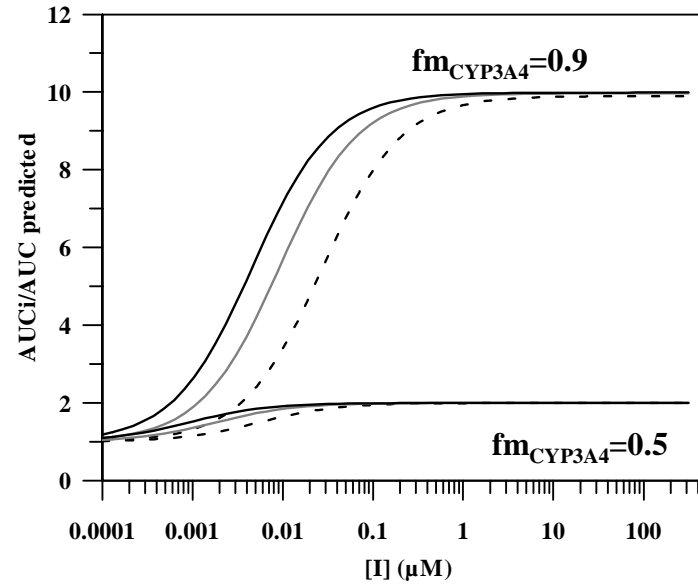


Figure 4

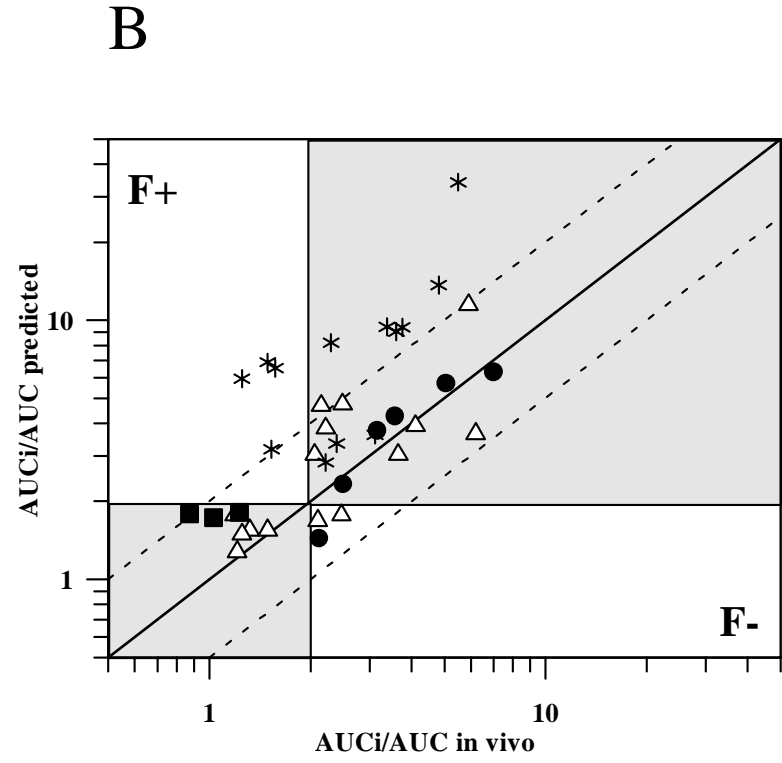
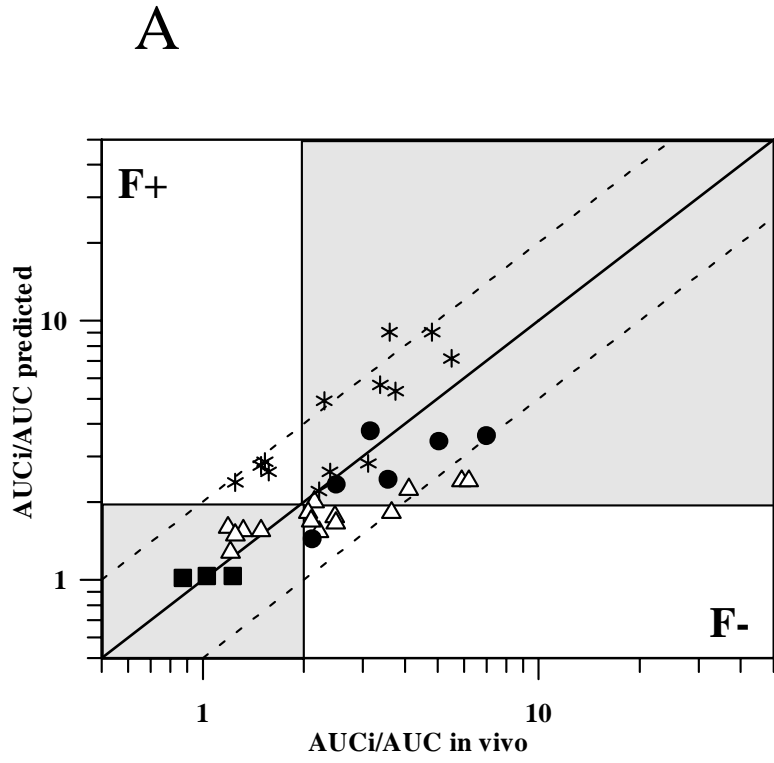


Figure 4

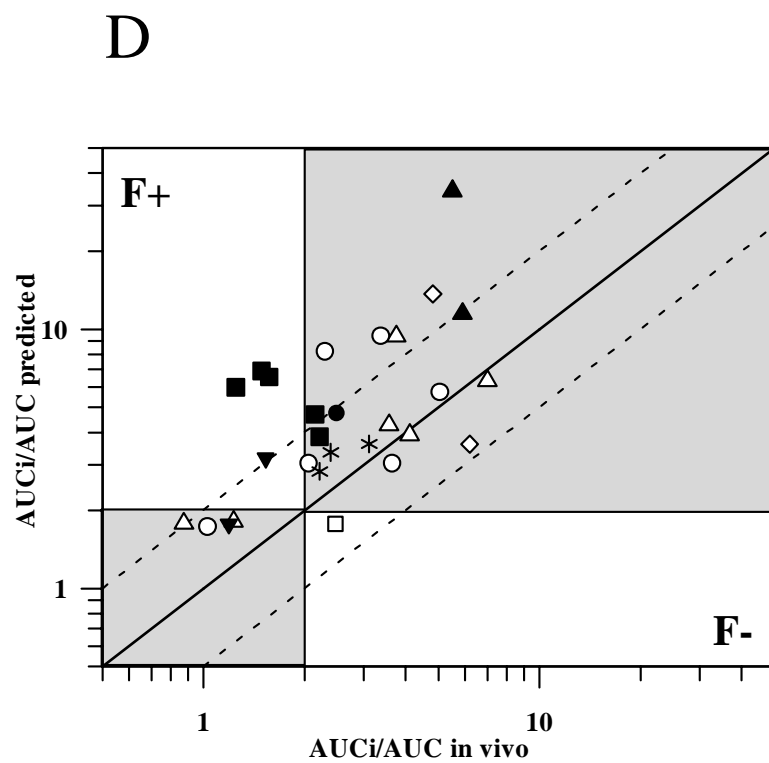
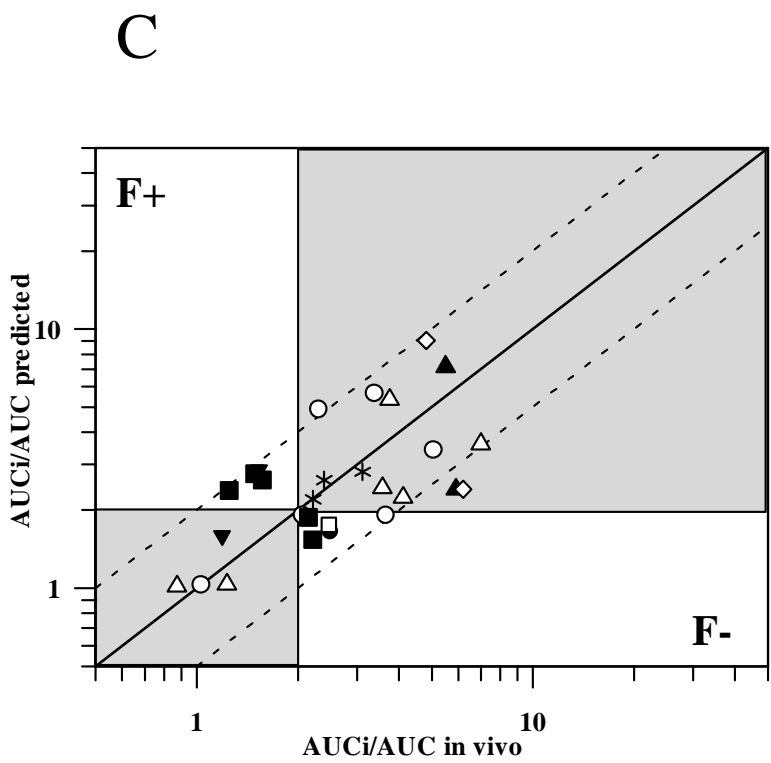




Figure 5

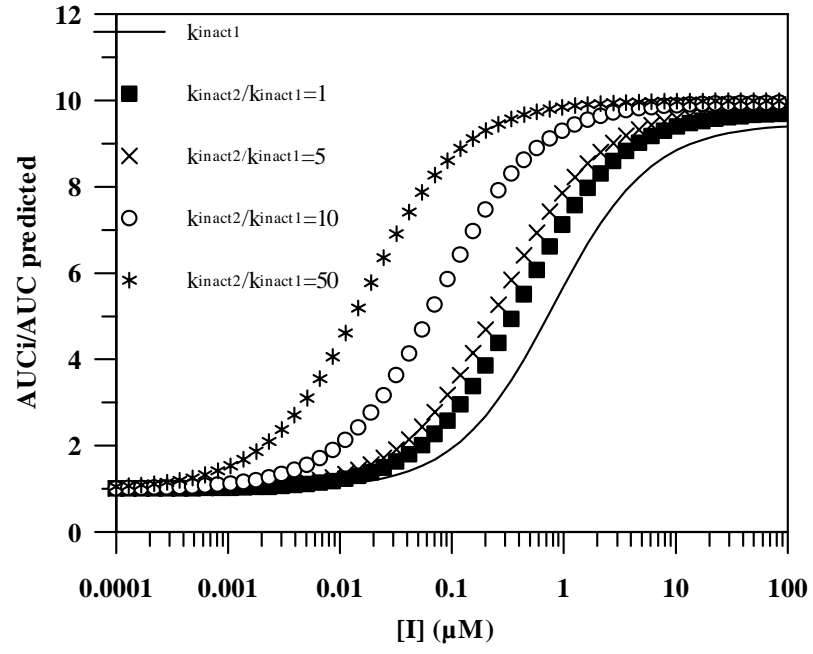


Figure 6

